



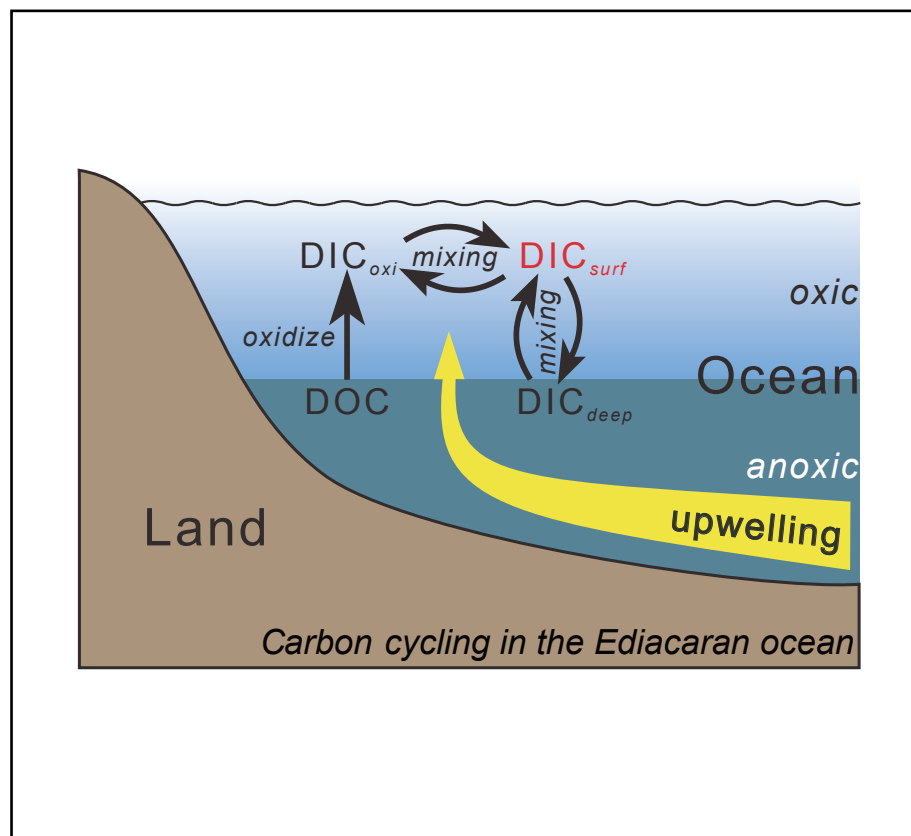
# Constraining the Ediacaran oceanic dissolved organic carbon reservoir: Insights from carbon isotopic records from a drill core from South China

Yunpei Gao, Yizhe Gong, and Xiaoyan Chen 

School of Earth and Space Sciences, University of Science and Technology of China, Hefei 230026, China

 Correspondence: Xiaoyan Chen, E-mail: [cxyan@ustc.edu.cn](mailto:cxyan@ustc.edu.cn)

## Graphical abstract




Carbon species conversions between dissolved inorganic carbon (DIC) and dissolved organic carbon (DOC) in the Ediacaran ocean.


## Public summary

- The micro-drilled and whole-rock  $\delta^{13}\text{C}_{\text{carb}}$  results for the Wangji drill core are well consistent, precluding severe authigenic carbonate influence.
- Negative  $\delta^{13}\text{C}_{\text{carb}}$  excursions indicate  $\sim 10^{19}$  mol oceanic DOC may have been oxidized.
- The decrease of DOC reservoir suggests a more oxygenated surface Earth (elevated atmospheric  $p\text{O}_2$  and/or oceanic  $[\text{SO}_4^{2-}]$ ) in the Ediacaran Period.

# Constraining the Ediacaran oceanic dissolved organic carbon reservoir: Insights from carbon isotopic records from a drill core from South China

Yunpei Gao, Yizhe Gong, and Xiaoyan Chen 

School of Earth and Space Sciences, University of Science and Technology of China, Hefei 230026, China

 Correspondence: Xiaoyan Chen, E-mail: [cxyan@ustc.edu.cn](mailto:cxyan@ustc.edu.cn)



Cite This: *JUSTC*, 2022, 52(2): 5 (11pp)



Read Online



Supporting Information

**Abstract:** The evolution of the atmospheric oxygen content through Earth's history is a key issue in paleoclimatic and paleoenvironmental research. There were at least two oxygenation events in the Precambrian that involved fundamental changes in both biotic innovation and the surface environment. However, a large dissolved organic carbon (DOC) pool maintained in deep oceans during the Neoproterozoic may have extended the time interval between the two oxygenation events. To test the DOC hypothesis, we conducted detailed micro-drilled analyses of carbonate carbon isotopes ( $\delta^{13}\text{C}_{\text{carb}}$ ) of a long Ediacaran drill core (the Wangji drill core), for which whole-rock  $\delta^{13}\text{C}_{\text{carb}}$  and organic carbon isotope ( $\delta^{13}\text{C}_{\text{org}}$ ) records were available. The micro-drilled  $\delta^{13}\text{C}_{\text{carb}}$  values obtained in this study are consistent with whole-rock  $\delta^{13}\text{C}_{\text{carb}}$  results, precluding the influence of severe authigenic carbonate incorporation. Importantly, the multiple negative  $\delta^{13}\text{C}_{\text{carb}}$  excursions in the Wangji drill core were likely linked with upwelling events, during which DOC was supplied to the surface water and oxidized. Using box models, we estimate that  $\sim 3.6 \times 10^{19}$  mol and  $\sim 2.0 \times 10^{19}$  mol DOC were converted to bicarbonate during two negative  $\delta^{13}\text{C}_{\text{carb}}$  excursions spanning millions of years. The estimations are approximately 1000 times the modern marine DOC reservoir. Our results support a relatively high oxidation capacity (elevated atmospheric  $p\text{O}_2$  and/or oceanic  $[\text{SO}_4^{2-}]$ ) of the Earth's surface during the early Ediacaran Period.

**Keywords:** oxygenation event; Ediacaran; South China; carbon isotopes; DOC; upwelling

**CLC number:** P593

**Document code:** A

## 1 Introduction

The oxygen in Earth's atmosphere and oceans has created a habitable planet, characterized by diverse life forms and complex ecosystems. The atmospheric oxygen content today is  $\sim 21\%$ , but it has varied throughout Earth's history. Numerous paleoenvironmental studies have revealed the occurrence of at least two major events of increasing atmospheric oxygen content at a very early stage in Earth's history<sup>[1–8]</sup>. The first oxygenation event occurred  $\sim 2450$ – $2200$  million years (Myr) ago<sup>[9]</sup>, known as the “Great Oxygenation Event (GOE)”, which witnessed an  $\text{O}_2$  rise above a threshold of at least  $10^{-5}$  of its present atmospheric level (PAL)<sup>[1, 3, 10]</sup> (Fig. 1). During this event, the atmospheric ozone layer that efficiently shields the Earth from much of the incoming solar ultraviolet radiation may have formed<sup>[11]</sup>. Additionally, the redox state of most shallow oceans may have changed from anoxic (dissolved oxygen deficient) to oxic (with dissolved oxygen)<sup>[12]</sup>, providing a more habitable environment for life. The second atmospheric oxygenation event is called the “Neoproterozoic Oxygenation Event (NOE)” and occurred  $\sim 750$ – $550$  Myr ago<sup>[5]</sup> (Fig. 1). During the NOE, atmospheric  $\text{O}_2$  level was further elevated, and the deep oceans may have experienced oxygenation<sup>[2, 6, 13]</sup>. Additionally, diverse macro-animal fossils, named the Ediacaran biota, have been dis-

covered in the Ediacaran strata (635–541 Myr ago) of different continents. Two key factors may have promoted the NOE. The first is the extremely high concentration of phosphate maintained in late Neoproterozoic seawater, which may have greatly stimulated the release of oxygen by aquatic primary productivity<sup>[14, 15]</sup>. The second is linked to the conversion of the dominant photosynthesizing species from cyanobacteria to

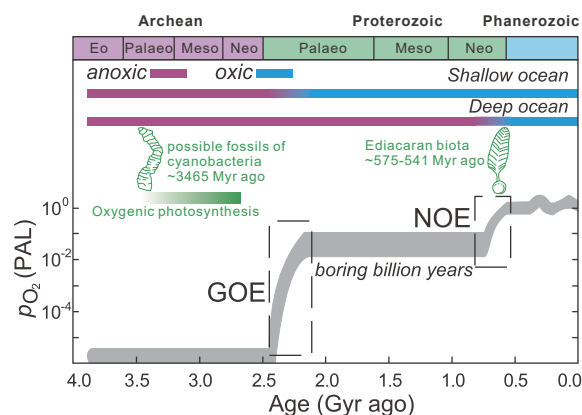


**Fig. 1.** Geological history of atmospheric oxygen and oceanic redox state.  $p\text{O}_2$ , atmospheric partial pressure of  $\text{O}_2$ ; PAL, present atmospheric level; Gyr, billion year; GOE, Great Oxygenation Event; NOE, Neoproterozoic Oxygenation Event.

algae<sup>[16]</sup>, the organic product of which has a higher burial efficiency<sup>[17]</sup> (Fig. 2).

The oxygen contents of the atmosphere and oceans between the GOE and NOE appear to have been relatively invariant (Fig. 1). Rothman et al.<sup>[18]</sup> proposed a distinct Neoproterozoic ocean model in which there was a gradual evolution to a high dissolved organic carbon (DOC) level under the dominance of cyanobacteria (Fig. 2a). With the immense DOC storage, the deep oceans were unable to become oxygenated until the radiation of algae in the late Neoproterozoic. One of the key pieces of evidence supporting the DOC hypothesis is the carbon isotopic records that are preserved in marine sediments (e.g., carbonates and shales). Carbon has two stable isotopes in nature, <sup>12</sup>C and <sup>13</sup>C, with abundances of 98.93% and 1.07%, respectively<sup>[19]</sup>. Isotopic compositions are often expressed as delta (δ) values, which represent the relative isotopic ratios compared with a chosen standard. For carbon, the isotopic composition is generally expressed as<sup>[19]</sup>

$$\delta^{13}\text{C} = \left[ \left( \frac{^{13}\text{C}/^{12}\text{C}}{\text{sample}} / \left( \frac{^{13}\text{C}/^{12}\text{C}}{\text{standard}} \right) - 1 \right) \times 1000 \right] \quad (1)$$

where the standard is the Vienna Peedee Belemnite (VPDB). The naturally occurring variations in carbon isotope composition can range from ~-100‰ to ~+20‰. Among numerous carbon-bearing species, two of the most important carbon reservoirs on the Earth's surface are marine carbonates and biogenic organic matter, with average δ<sup>13</sup>C values of ~0‰ (carbonate carbon isotopes; δ<sup>13</sup>C<sub>carb</sub>) and ~-25‰ (organic carbon isotopes; δ<sup>13</sup>C<sub>org</sub>). For the Phanerozoic (541 Myr ago to present), the photosynthesis-dominated carbon cycle led to roughly parallel δ<sup>13</sup>C<sub>carb</sub> and δ<sup>13</sup>C<sub>org</sub> records in sedimentary rocks<sup>[20,21]</sup>. However, Neoproterozoic δ<sup>13</sup>C<sub>carb</sub> and δ<sup>13</sup>C<sub>org</sub> records show significant differences from those of the Phanerozoic. First, multiple large negative δ<sup>13</sup>C<sub>carb</sub> excursions have been observed in Neoproterozoic carbonates<sup>[22]</sup>. Many of these negative δ<sup>13</sup>C<sub>carb</sub> values are well below the isotopic values of

volcanic CO<sub>2</sub> (-6‰), which cannot be solely interpreted in terms of the classical photosynthesis-dominated carbon cycle. These negative δ<sup>13</sup>C<sub>carb</sub> values are speculated to have resulted from the intermittent oxidation of oceanic DOC with extremely low δ<sup>13</sup>C values<sup>[2,13,18]</sup>. Second, the contemporaneous δ<sup>13</sup>C<sub>org</sub> records remain relatively constant and are completely decoupled from the δ<sup>13</sup>C<sub>carb</sub> records. Therefore, the decoupled relationship between δ<sup>13</sup>C<sub>carb</sub> and δ<sup>13</sup>C<sub>org</sub> in early Neoproterozoic sedimentary strata may indicate the buffering effect of δ<sup>13</sup>C<sub>org</sub> induced by a large DOC pool, starting at ~720–635 Myr ago in the Cryogenian Period<sup>[23]</sup>, and ending at ~550 Myr ago in the late Ediacaran Period<sup>[2,13]</sup>.

In addition to the DOC hypothesis, Schrag et al.<sup>[24]</sup> proposed another mechanism, authigenic carbonate, to account for the unique Neoproterozoic carbon isotopic records. Authigenic carbonates are generally associated with anaerobic bacterial metabolism at the sediment-water interface or within sediment pore waters that may have extremely negative δ<sup>13</sup>C<sub>carb</sub> values<sup>[25]</sup>. They are proposed to have been widespread in the anoxic ocean floor and have contributed to Precambrian negative δ<sup>13</sup>C<sub>carb</sub> excursions<sup>[24]</sup>. This hypothesis is supported by observations of authigenic carbonate cements, as well as by micro-drilled isotopic results (as low as -35‰) in intervals of negative δ<sup>13</sup>C<sub>carb</sub> in late Neoproterozoic strata from South China<sup>[26,27]</sup>. The mixing of authigenic carbonate cements may obscure the primary environmental information and complicate the classical interpretation of sedimentary δ<sup>13</sup>C<sub>carb</sub> records. Therefore, the influence of the authigenic carbonate Neoproterozoic carbon cycle should be assessed with caution.

To further examine the DOC and authigenic carbonate hypotheses, more high-resolution δ<sup>13</sup>C<sub>carb</sub> and δ<sup>13</sup>C<sub>org</sub> records for the Neoproterozoic are needed. In addition, micro-drilled analyses of δ<sup>13</sup>C<sub>carb</sub> should be applied to the excursion intervals initially defined by whole-rock δ<sup>13</sup>C<sub>carb</sub> records. In this study, we conducted micro-drilled analyses of δ<sup>13</sup>C<sub>carb</sub> from a long drill core, for which the whole-rock δ<sup>13</sup>C<sub>carb</sub> and δ<sup>13</sup>C<sub>org</sub> records for the entire Ediacaran Period have already been reported<sup>[28,29]</sup>. By comparing the micro-drilled and whole-rock δ<sup>13</sup>C<sub>carb</sub> results, we assessed the contribution of authigenic carbonate to the negative δ<sup>13</sup>C<sub>carb</sub> excursions in the drill core. Furthermore, by modeling a dynamic upwelling scenario based on δ<sup>13</sup>C<sub>carb</sub> and δ<sup>13</sup>C<sub>org</sub> compilations, we attempted to estimate the mass of DOC in the early Ediacaran ocean.

## 2 Geology, lithology, and chemostratigraphy of the Wangji drill core

### 2.1 Geological background and lithology

South China has preserved successive, massive late Neoproterozoic sedimentary rocks that provide a window for exploring the environmental conditions of the Precambrian. South China is composed of the Yangtze and Cathaysia blocks<sup>[30,31]</sup> (Fig. 3a). During the Ediacaran Period (635–541 Myr ago), the Yangtze Block was an oceanic setting consisting of inner shelf, intrashelf basin, shelf margin, slope, and deep basin environments<sup>[32]</sup> (Fig. 3b). We conducted a drilling project and obtained a long (~711 m) continuous drill core for

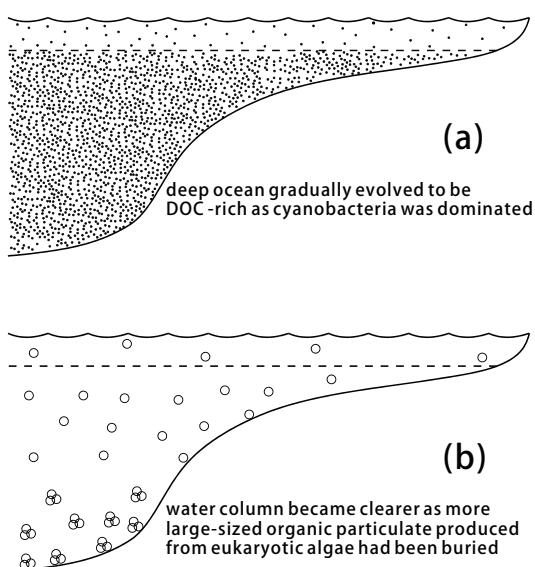


**Fig. 2.** Schematic diagrams of two dominant primary producers regulating the marine organic carbon cycle, modified after Butterfield<sup>[17]</sup>. (a) Cyanobacteria-dominated oceans. (b) Algae-dominated oceans. DOC, dissolved organic carbon.

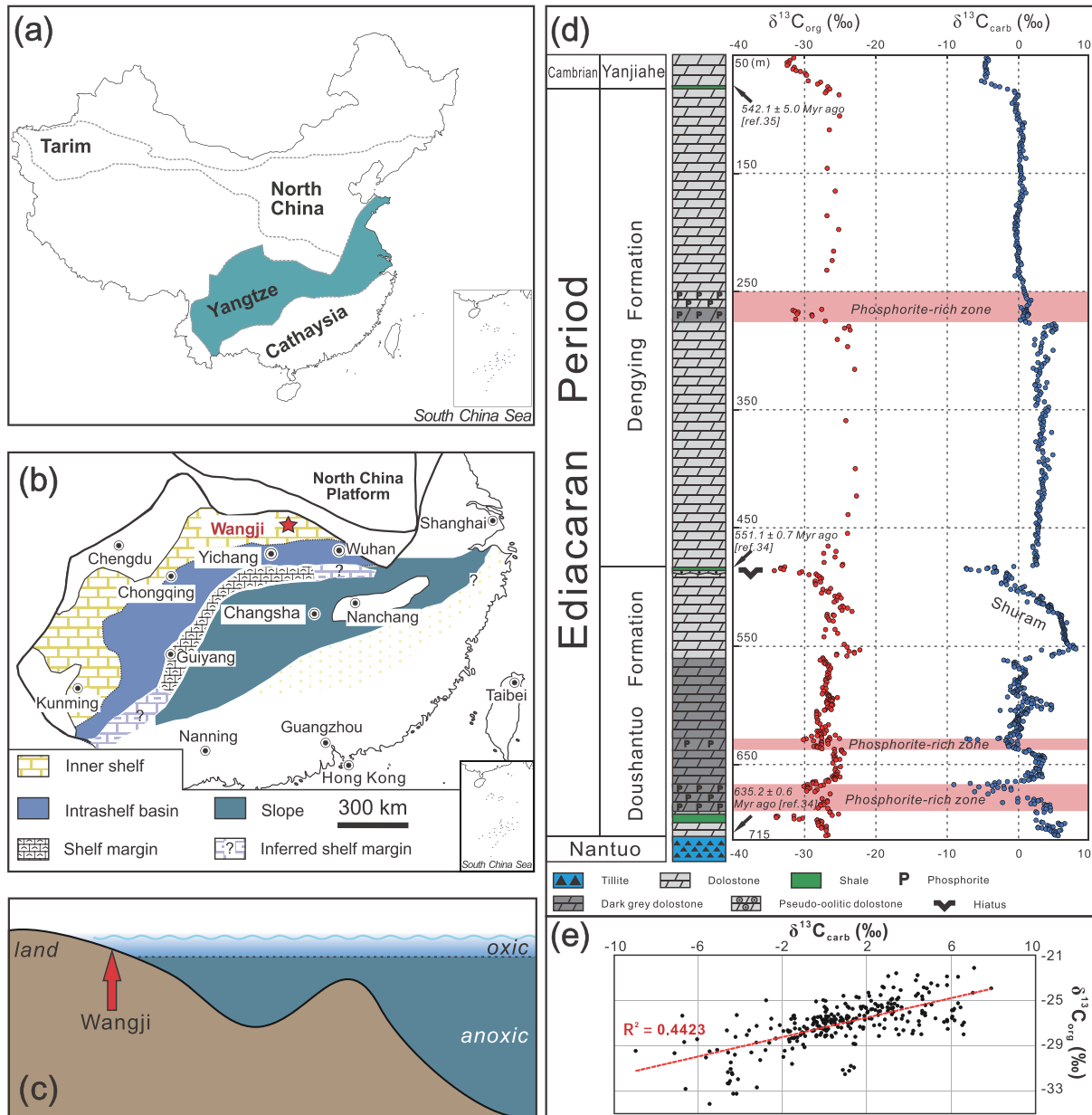


**Fig. 3.** (a) Generalized geological map of China. (b) Paleogeographic reconstruction of the Yangtze platform (South China) consisting of different facies associations during the Ediacaran, modified after Jiang et al.<sup>[32]</sup>. The red star marks the location of the Wangji drill core. (c) Transect from north to south in the Yangtze platform and the location of the Wangji drill core. (d) Lithostratigraphic, whole-rock  $\delta^{13}\text{C}_{\text{carb}}$ , and  $\delta^{13}\text{C}_{\text{org}}$  profiles of the Wangji drill core. The pink shading represents phosphorite-rich intervals. The ages are based on U/Pb dating by Condon et al.<sup>[34]</sup> and Chen et al.<sup>[35]</sup>. (E) Cross-plot of the whole-rock  $\delta^{13}\text{C}_{\text{carb}}$  and  $\delta^{13}\text{C}_{\text{org}}$  values of the Wangji drill core.

the entire Ediacaran Period from Wangji town, Hubei Province (Fig. 3b). Based on paleogeographic reconstructions, the Wangji drill core was deposited in the very shallow region of an inner intra-basin<sup>[28, 29, 33]</sup> (Fig. 3c). The Ediacaran strata in the Wangji drill core can be subdivided into the Doushantuo Formation (635–551 Myr ago) and the Dengying Formation (551–541 Myr ago)<sup>[34, 35]</sup> (Fig. 3d). The Doushantuo Formation overlies the Cryogenian Nantuo tillite, which corresponds to the widespread glacial deposits of the global “Marinoan” glaciation. The Doushantuo Formation (710.3–483.0 m) is composed of dolomite, phosphorite, and black shale, while the Dengying Formation (483.0–78.9 m) is mainly composed of dolomite. Although the Dengying Form-

ation was only deposited for ~10 Myr, it is much thicker than the Doushantuo Formation (~84 Myr). The topmost part of the Wangji drill core is the Cambrian Yanjiahe Formation, which is characterized by shale and dolomite (Fig. 3d).

## 2.2 Summary of whole-rock $\delta^{13}\text{C}_{\text{carb}}$ and $\delta^{13}\text{C}_{\text{org}}$ results for the Wangji drill core

We had previously conducted high-resolution, whole-rock  $\delta^{13}\text{C}_{\text{carb}}$  and  $\delta^{13}\text{C}_{\text{org}}$  analyses of the Wangji drill core<sup>[28, 29]</sup>. The  $\delta^{13}\text{C}_{\text{carb}}$  values range from -8.95‰ to +8.16‰ and reveal multiple large positive and negative excursions<sup>[28]</sup> (Fig. 3d). The  $\delta^{13}\text{C}_{\text{carb}}$  results are roughly consistent with the  $\delta^{13}\text{C}_{\text{carb}}$  records from other sections in South China<sup>[13, 36–38]</sup>. Notably, two negat-



ive  $\delta^{13}\text{C}_{\text{carb}}$  excursion intervals (as low as  $-8.95\%$ , 684.2–660.6 m; and  $-7.11\%$ , 642.2–621.8 m) are closely associated with phosphorites in the lower part of the Doushantuo Formation. In addition, the global “Shuram-Wonoka” negative  $\delta^{13}\text{C}_{\text{carb}}$  excursion (from  $-7.20\%$  to  $8.16\%$ , 552.4–481.8 m) has also been identified in the upper part of the Doushantuo Formation, enabling stratigraphic correlations among continents.

The  $\delta^{13}\text{C}_{\text{org}}$  values for the Wangji drill core range from  $-34.12\%$  to  $-22.13\%$ , and show a similar trend of variation to the  $\delta^{13}\text{C}_{\text{carb}}$  record, although the magnitude of each excursion is relatively small<sup>[29]</sup> (Fig. 3d). The  $\delta^{13}\text{C}_{\text{org}}$  results for the Wangji drill core are very different from those of other sections in South China, such as the Jiulongwan<sup>[13]</sup> and Siduping<sup>[39]</sup> sections, where relatively invariant  $\delta^{13}\text{C}_{\text{org}}$  profiles are recognized and are completely decoupled from their  $\delta^{13}\text{C}_{\text{carb}}$  profiles. In contrast, the Wangji  $\delta^{13}\text{C}_{\text{carb}}$  and  $\delta^{13}\text{C}_{\text{org}}$  values showed a weak positive correlation, indicative of a “semi-coupled” relationship (Fig. 3e).

### 3 Methods

First, thin sections of representative rock samples from the Wangji drill core were prepared for detailed petrographic observations to assess potential diagenetic effects, such as the occurrence of authigenic cements and veins. The rock samples were then polished using sandpaper of different grades, and the polished surfaces were further scanned as high-resolution photos. A portable dental drill was used to ob-

tain the microdrilled powder samples from the polished surfaces. Each microsampling area was less than  $1\text{ mm} \times 1\text{ mm}$ . The weighed powder samples were then placed in a glass vial and reacted with concentrated  $\text{H}_3\text{PO}_4$  in pre-vacuum conditions in a Thermo Scientific Kiel IV Carbonate Device. The liberated  $\text{CO}_2$  was purified in multiple cryogenic traps and finally transferred to a Thermo Scientific MAT 253 gas mass spectrometer for the determination of C and O isotopic compositions. The C and O isotopic compositions are reported as per mil ( $\%$ ) deviation relative to the VPDB. Based on routine analyses of standard samples GBW04416 and GBW04417, the reproducibility was better than  $0.05\%$  for  $\delta^{13}\text{C}$ , and better than  $0.08\%$  for  $\delta^{18}\text{O}$ .

### 4 Results

Thin-section petrographic observations indicate that the samples are mostly micritic to fine crystalline dolomites, and no obvious authigenic cements or carbonate veins are evident (Fig. 4). A total of 161 micro-sampling C and O isotopic compositions of 48 polished rocks from the Wangji drill core were obtained (Figs. 5–8). Most of the polished rock surfaces also show microcrystalline features (Figs. 5–8). The micro-sampling  $\delta^{13}\text{C}_{\text{carb}}$  values range from  $-9.83\%$  to  $8.52\%$ , and in each sample, the micro-sampling values are roughly consistent with the whole-rock  $\delta^{13}\text{C}_{\text{carb}}$  values (Figs. 5–9). The micro-sampling  $\delta^{18}\text{O}_{\text{carb}}$  results range from  $-12.48\%$  to  $-1.95\%$ . However, in each sample, the micro-sampling  $\delta^{18}\text{O}_{\text{carb}}$  values show a much larger range of variation than the whole-rock

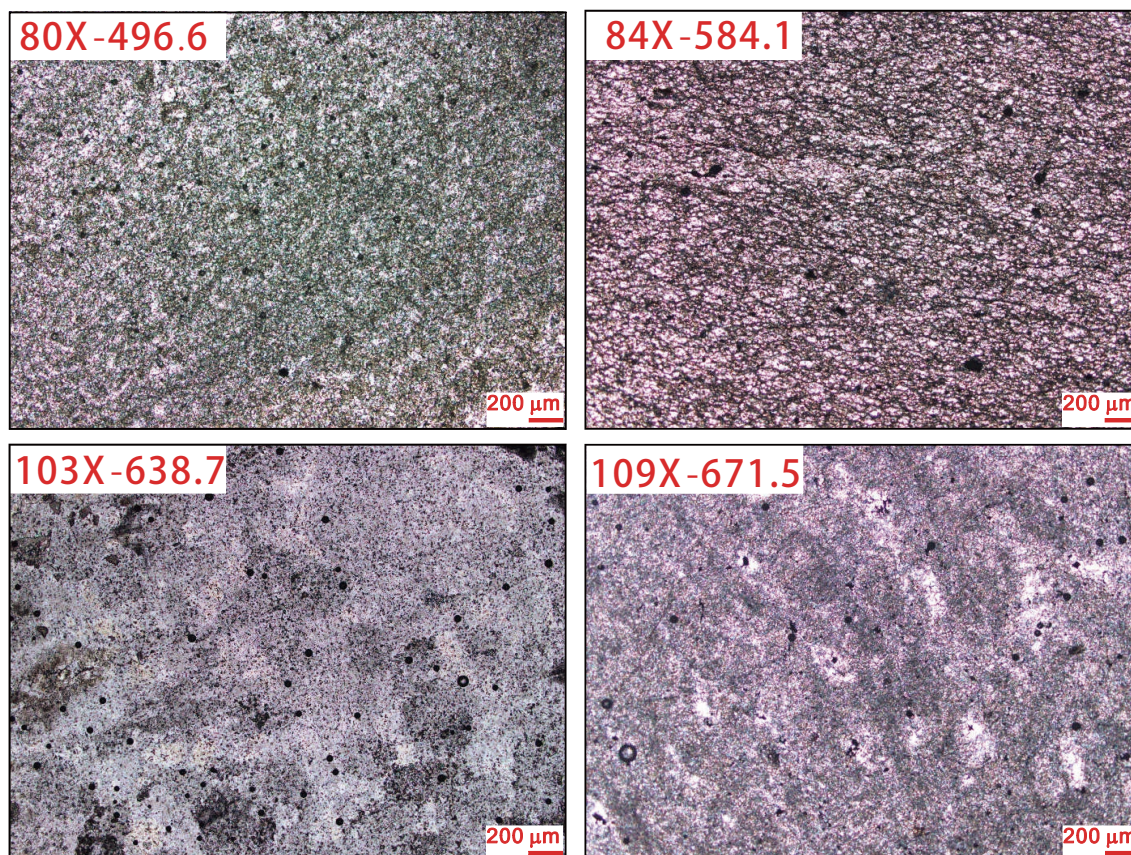
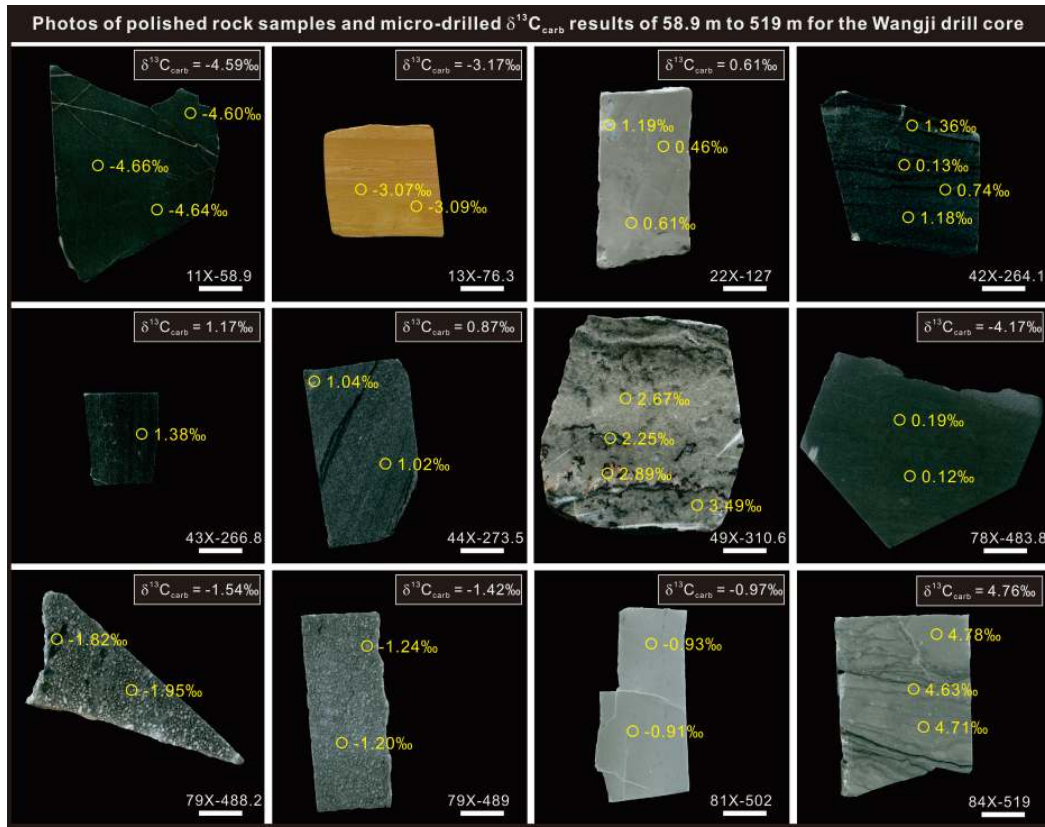
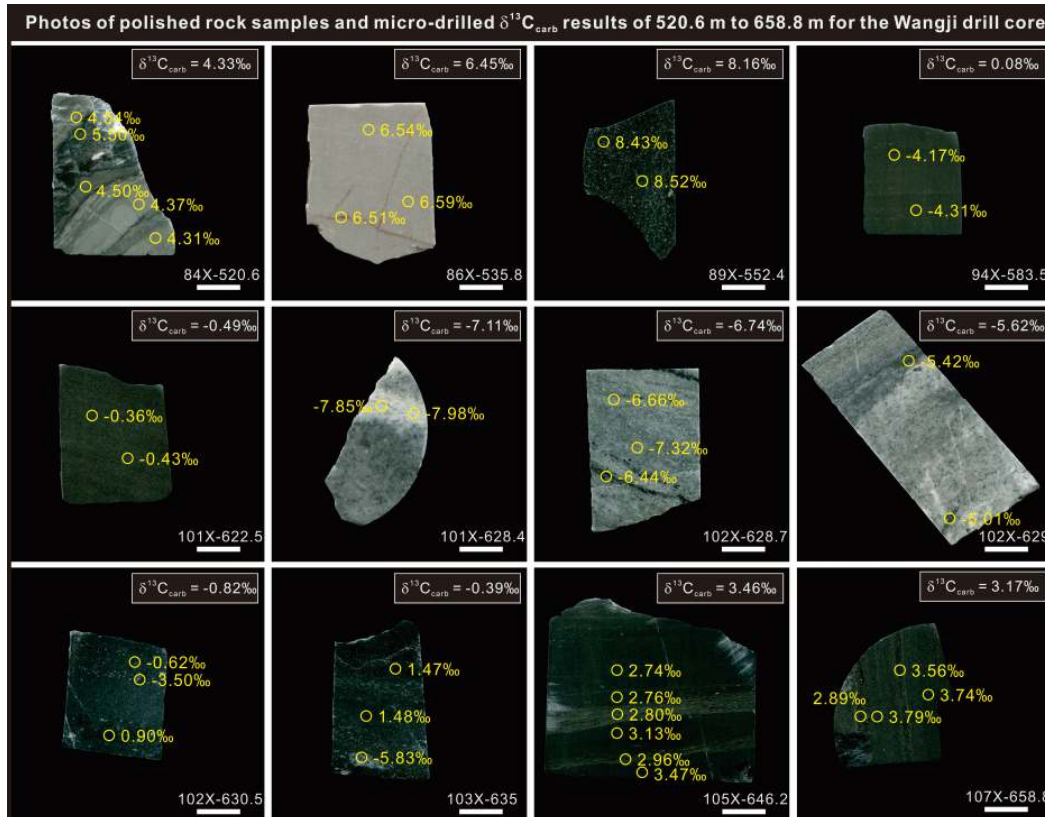


Fig. 4. Representative single polarizing microscope photos of thin sections from the Wangji drill core.





**Fig. 5.** Photos of polished rock samples and micro-drilled  $\delta^{13}\text{C}_{\text{carb}}$  results of the interval 58.9–519 m in the Wangji drill core. The whole-rock  $\delta^{13}\text{C}_{\text{carb}}$  value is on the upper right corner, and the white scale bar in the bottom right corner is 1 cm.



**Fig. 6.** Photos of polished rock samples and micro-drilled  $\delta^{13}\text{C}_{\text{carb}}$  results for the interval 520.6–658.8 m in the Wangji drill core. The whole-rock  $\delta^{13}\text{C}_{\text{carb}}$  value is on the upper right corner, and the white scale bar in the bottom right corner is 1 cm.

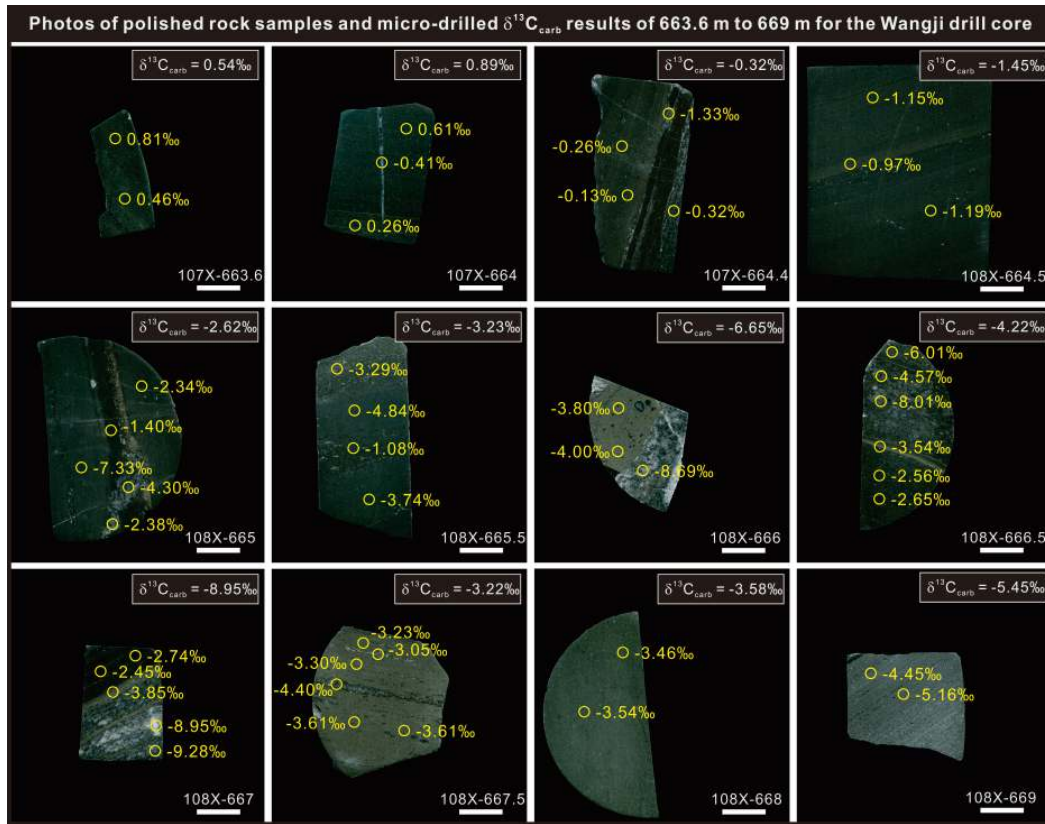


**Fig. 7.** Photos of polished rock samples and micro-drilled  $\delta^{13}\text{C}_{\text{carb}}$  results for the interval 663.6–669 m in the Wangji drill core. The whole-rock  $\delta^{13}\text{C}_{\text{carb}}$  value is in the upper right corner, and the white scale bar in the bottom right corner is 1 cm.

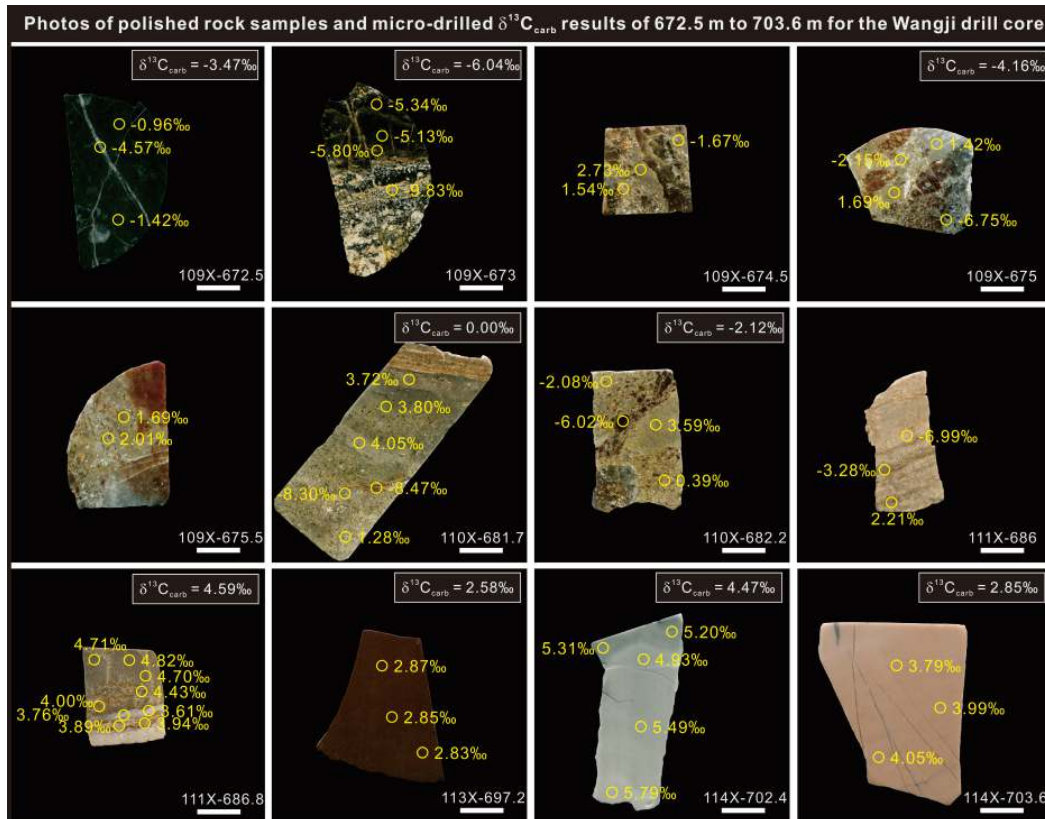


**Fig. 8.** Photos of polished rock samples and micro-drilled  $\delta^{13}\text{C}_{\text{carb}}$  results for the interval 672.5–703.6 m in the Wangji drill core. The whole-rock  $\delta^{13}\text{C}_{\text{carb}}$  value is on the upper right corner, and the white scale bar in the bottom right corner is 1 cm.

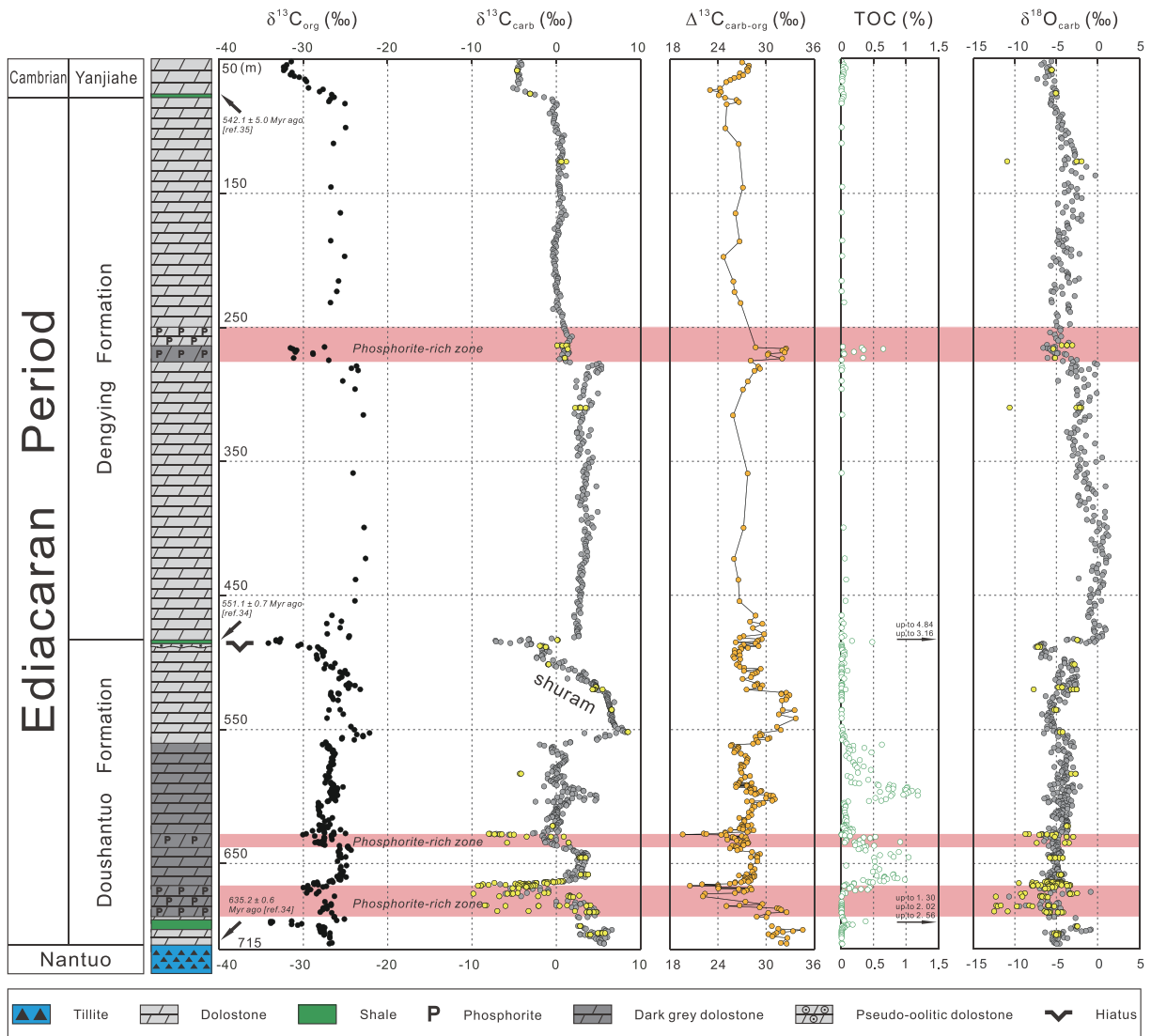


**Fig. 9.**  $\delta^{13}\text{C}_{\text{org}}$ ,  $\delta^{13}\text{C}_{\text{carb}}$ ,  $\Delta^{13}\text{C}_{\text{carb-org}}$ , total organic carbon content (TOC), and  $\delta^{18}\text{O}_{\text{carb}}$  profiles for the Wangji drill core. Yellow points represent micro-drilled  $\delta^{13}\text{C}_{\text{carb}}$  and  $\delta^{18}\text{O}_{\text{carb}}$  results obtained in this study. The pink shading represents phosphorite-rich intervals. The ages are based on U/Pb dating by Condon et al.<sup>[34]</sup> and Chen et al.<sup>[35]</sup>.

$\delta^{18}\text{O}_{\text{carb}}$  values, potentially reducing the paleoenvironmental significance of the oxygen isotopic records (Fig. 9).

## 5 Discussion

### 5.1 Contribution of authigenic carbonates to the whole-rock negative $^{13}\text{C}_{\text{carb}}$ excursions in the Wangji drill core

Most modern carbonates are biogenic and are derived from the stacking of the hard body parts of corals, sponges, and foraminifers<sup>[40]</sup>. Carbonates can also be precipitated chemically in seawater and occupy a substantial proportion of Precambrian oceans where reef-building organisms had not yet evolved. The carbon sources of both biogenic and chemical carbonates are bicarbonate ions dissolved in seawater. Because the C isotopic composition of dissolved bicarbonate ions is relatively uniform and the isotopic fractionation between the bicarbonate ion and carbonate minerals is generally less than 2‰<sup>[21]</sup>,

the  $\delta^{13}\text{C}$  signals of these carbonates have been suggested to record the global C isotopic compositions of marine bicarbonate ions in the past.

As mentioned above, authigenic carbonates are formed in anoxic zones where the local alkalinity is expected to be rapidly elevated owing to organic matter remineralization<sup>[24]</sup>. Therefore, authigenic carbonates are formed during the very early diagenetic stage, and their  $\delta^{13}\text{C}_{\text{carb}}$  signals mostly reflect the C isotopic compositions of organic matter, rather than that of the dissolved bicarbonate ion. Because authigenic carbonates are extremely depleted in  $^{13}\text{C}$ , their widespread burial was proposed to account for the large  $\delta^{13}\text{C}_{\text{carb}}$  records preserved in Precambrian strata<sup>[24]</sup>. Recent studies have identified authigenic carbonate cements in the “Shuram-Wonoka” negative  $\delta^{13}\text{C}_{\text{carb}}$  excursion interval, emphasizing the contribution of authigenic carbonate to whole-rock  $\delta^{13}\text{C}_{\text{carb}}$  excursions<sup>[26,27]</sup>. In these samples, the authigenic carbonate cements are typically white, and their  $\delta^{13}\text{C}_{\text{carb}}$  values differ substantially from those



of the surrounding primary carbonates. Therefore, the whole-rock  $\delta^{13}\text{C}_{\text{carb}}$  values may reflect mixing signals between authigenic carbonate and primary carbonate that complicate their paleoenvironmental interpretation. Additionally, these authigenic carbonate cements are likely to be formed with phosphorites, because phosphate is readily redistributed via organic matter remineralization by sulfate-reducing bacteria.

In the Wangji drill core, three negative  $\delta^{13}\text{C}_{\text{carb}}$  excursions are closely associated with phosphorites, two in the lower Doushantuo Formation and one in the middle Dengying Formation. Authigenic carbonates may therefore also be present in these layers and contribute to whole-rock negative  $\delta^{13}\text{C}_{\text{carb}}$  excursions. However, based on petrographic observations of polished rock samples and thin sections, the carbonates are mostly micritic to fine crystalline dolomites with a light or dark grey color and lack typical authigenic carbonate features (Figs. 4–8). In addition, the micro-drilled  $\delta^{13}\text{C}_{\text{carb}}$  values show good consistency with the whole-rock  $\delta^{13}\text{C}_{\text{carb}}$  results, with the absence of extremely negative  $\delta^{13}\text{C}_{\text{carb}}$  values ( $<-10\%$ ) (Fig. 9). Moreover, the whole-rock negative  $\delta^{13}\text{C}_{\text{carb}}$  excursions in the Wangji drill core can be well correlated on the basinal scale<sup>[28]</sup>. Lastly, the similar trend of variation of  $\delta^{13}\text{C}_{\text{carb}}$  and  $\delta^{13}\text{C}_{\text{org}}$  also indicates minor authigenic incorporation, even in these phosphorite-rich layers (Fig. 9). Therefore, it is reasonable to conclude that the  $\delta^{13}\text{C}_{\text{carb}}$  values for the Wangji drill are more likely to record the primary isotopic information of the Ediacaran seawater bicarbonate ion.

### 5.2 Seawater upwelling model and semi-coupled $\delta^{13}\text{C}_{\text{carb}}$ and $\delta^{13}\text{C}_{\text{org}}$ records

What caused the large negative  $\delta^{13}\text{C}_{\text{carb}}$  excursions in the Wangji drill core? We have previously proposed a seawater upwelling model to interpret the synchronous occurrence of negative  $\delta^{13}\text{C}_{\text{carb}}$  excursions and phosphorite deposits<sup>[28,29]</sup>. The incursion of anoxic deep seawater into shelf regions supplies large amounts of phosphate, deep-water dissolved inorganic carbon (DIC) and DOC to shallow water. On one hand, the incorporation of  $^{13}\text{C}$ -depleted DIC and subsequent oxidation of DOC would affect the original inorganic  $\delta^{13}\text{C}$  shallow water signal, ultimately resulting in negative  $\delta^{13}\text{C}_{\text{carb}}$  excursions. On the other hand, phosphate was much more readily precipitated via adsorption by ferric (hydr)oxide or binding with organic matter particles when the surrounding water body was oxic.

Most  $\delta^{13}\text{C}_{\text{org}}$  results from other sections in South China and elsewhere (e.g., Oman) show complete decoupling from the  $\delta^{13}\text{C}_{\text{carb}}$  record below the “Shuram-Wonoka” negative  $\delta^{13}\text{C}_{\text{carb}}$  excursion, but with a recovered co-variation at the end of the “Shuram-Wonoka” interval<sup>[2,13]</sup>. In the Wangji drill core, however, the  $\delta^{13}\text{C}_{\text{org}}$  results are only weakly coupled with the  $\delta^{13}\text{C}_{\text{carb}}$  record, even below the “Shuram-Wonoka” interval (Figs. 3d, 3e). The unique  $\delta^{13}\text{C}_{\text{org}}$  results of the Wangji drill core are consistent with the upwelling model proposed above. Owing to excess phosphate incorporation into shallow seawater, blooms of cyanobacteria and algae would generate sufficient organic matter to rival the DOC introduced by upwelling. In this case, the  $\delta^{13}\text{C}_{\text{org}}$  results for the Wangji drill core are likely to record geochemical mixing signals between

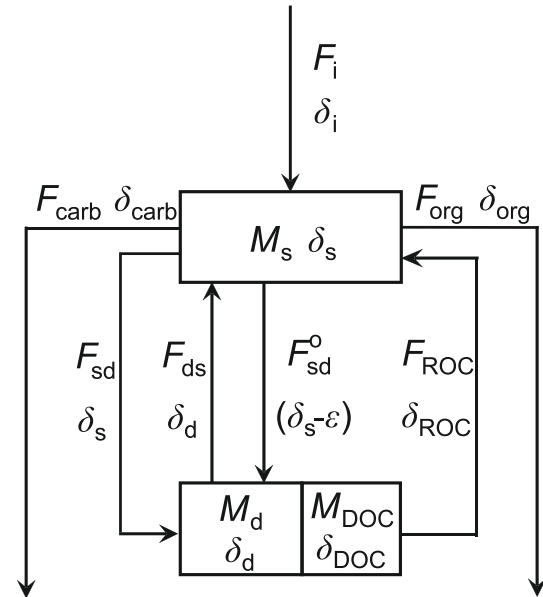


**Fig. 10.** Simple reservoir model of oceanic C cycling.  $M_s$  is the mass of the surface ocean DIC with the C isotope composition of  $\delta_s$ ;  $M_d$  is the mass of the deep ocean DIC with the C isotope composition of  $\delta_d$ ;  $M_{\text{DOC}}$  represents the mass of the deep ocean DOC with the C isotope composition of  $\delta_{\text{DOC}}$ ;  $F_i$  represents inputs of carbon from continental weathering, with an average isotopic composition of  $\delta_i$ ;  $F_{\text{ds}}$  is the inorganic carbon flux from the surface to the deep ocean;  $F_{\text{sd}}$  is the organic carbon flux from the surface to the deep ocean;  $F_{\text{ROC}}$  is the carbon flux from the remineralization of upwelled organic carbon, with the isotopic composition of  $\delta_{\text{ROC}}$ ;  $F_{\text{carb}}$  is the carbonate burial flux; and  $F_{\text{org}}$  is the organic carbon burial flux.

a major primary organic matter component and the DOC component. Thus, the  $\delta^{13}\text{C}_{\text{carb}}$  and  $\delta^{13}\text{C}_{\text{org}}$  records for the Wangji drill core potentially provide an opportunity to quantitatively estimate the size of the oceanic DOC storage at that time.

### 5.3 Quantitative estimation of the magnitude of the DOC reservoir in the early Ediacaran oceans

We used the paired  $\delta^{13}\text{C}_{\text{carb}}$  and  $\delta^{13}\text{C}_{\text{org}}$  values, integrated with a numerical model, to quantitatively evaluate the size of the DOC reservoir and its mechanistic links with carbon cycling during the late Neoproterozoic. The model includes three boxes, representing the surface ocean DIC, with reservoir size  $M_s$ , the deep ocean DIC, with reservoir size  $M_d$ , and the deep ocean DOC, with reservoir size  $M_{\text{DOC}}$ <sup>[41,42]</sup> (Fig. 10). The flux of DOC from the surface to deep water is ignored because its magnitude is negligible compared to that of the DOC reservoir. In the calculations, we also ignored the small C isotopic fractionation during carbonate mineral precipitation<sup>[41]</sup>. Since this upwelling scenario is a non-steady state, for all times ( $t$ ), the overall mass balance can be expressed as

$$dM_s/dt = F_i + F_{\text{ds}} + F_{\text{ROC}} - F_{\text{sd}} - F_{\text{sd}}^o - F_{\text{carb}} - F_{\text{org}} \quad (2)$$

where  $F_i$  is the average input flux of continental weathering,  $F_{\text{ds}}$  is the flux of deep ocean DIC transferred to the surface ocean,  $F_{\text{ROC}}$  is the flux of upwelled DOC that was oxidized to inorganic carbon in the surface ocean,  $F_{\text{sd}}$  is the flux of surface ocean DIC transferred to the deep ocean,  $F_{\text{sd}}^o$  is the flux of surface ocean organic matter that was remineralized to

deep ocean DIC,  $F_{carb}$  is the flux of carbonate burial, and  $F_{org}$  is the flux of organic carbon burial.

The isotopic mass balance can be expressed as

$$d(M_s \delta_s)/dt = F_i \delta_i + F_{ds} \delta_d + F_{ROC} \delta_{ROC} - F_{sd} \delta_s - F_{sd}^o (\delta_s - \varepsilon) - F_{carb} \delta_{carb} - F_{org} \delta_{org} \quad (3)$$

where  $\delta_s$  is the carbon isotopic value of surface ocean DIC,  $\delta_i$  is the average carbon isotopic value of continental weathering material,  $\delta_d$  is the carbon isotopic value of deep ocean DIC,  $\delta_{ROC}$  is the carbon isotopic value of the input flux from the remineralization of upwelled organic carbon (assuming no isotopic fractionation during remineralization, thus  $\delta_{ROC} = \delta_{DOC}$ ),  $\varepsilon$  refers to isotopic fractionation between DIC and organic carbon, and  $\delta_{carb}$  and  $\delta_{org}$  are carbon isotopic values of carbonate and organic matter, respectively.

Eq.(3) can be reformulated using Eq.(2) and the product rule of calculus, to explicitly show the factors controlling the isotopic composition of the surface ocean ( $\delta_s$ ) reservoir:

$$d\delta_s/dt = [F_i (\delta_i - \delta_s) + F_{ds} (\delta_d - \delta_s) + F_{ROC} (\delta_{ROC} - \delta_s) + (F_{org} + F_{sd}^o) \varepsilon] / M_s \quad (4)$$

Our focus is mainly on the phosphorite-rich layers of the lower Doushantuo Formation. Below the first negative  $\delta^{13}C_{carb}$  excursion (from  $-8.95\%$  to  $4.49\%$ , 684.2–660.6 m), the  $\delta^{13}C_{carb}$  values are almost constant at  $\sim 5\%$ , which can be regarded as the baseline of the original shallow-water  $\delta^{13}C_{carb}$  values. When upwelling events occurred, deep-water DIC and

the oxidation of DOC to DIC were mixed with the original shallow-water DIC, resulting in the first negative  $\delta^{13}C_{carb}$  excursion. After the upwelling events, the  $\delta^{13}C_{carb}$  values gradually recovered and became positive, but with the baseline changing from  $\sim 5\%$  and  $\sim 3\%$ . A similar scenario can be applied to the second negative  $\delta^{13}C_{carb}$  excursion (from  $-7.11\%$  to  $2.98\%$ , 642.2–621.8 m). The C isotopic compositions of deep-water DIC and DOC can be estimated as  $-1\%$  and  $-30\%$ , respectively, when considering the  $\delta^{13}C_{carb}$  and  $\delta^{13}C_{org}$  records of the deeper Jiulongwan section<sup>[13,43]</sup>. Other important parameters are listed in Table 1.

The simulation results (Fig. 11) show that the two negative  $\delta^{13}C_{carb}$  excursions in the lower Doushantuo Formation are well modeled by an intermittent upwelling scenario. The upwelling events could have persisted for several million years

**Table 1.** Parameters used in the C cycling model.

Model parameter	Value	Reference
$F_i$	$2.5 \times 10^{19} \text{ mol} \cdot \text{Myr}^{-1}$	Gill et al. <sup>[44]</sup>
$\delta_i$	$-5\%$	Shi et al. <sup>[43]</sup>
$M_s$	$6 \times 10^{18} \text{ mol}$	Gill et al. <sup>[44]</sup>
$F_{sd}^o$	$2 \times 10^{17} \text{ mol} \cdot \text{Myr}^{-1}$	
$F_{ds}$	$1.2 \times 10^{18} \text{ mol} \cdot \text{Myr}^{-1}$	
$\delta_d$	$-1\%$	McFadden et al. <sup>[13]</sup>
$\varepsilon$	$28\% - 30\%$	Hayes et al. <sup>[21]</sup>
$\delta_{DOC}$	$-30\%$	Shi et al. <sup>[43]</sup>

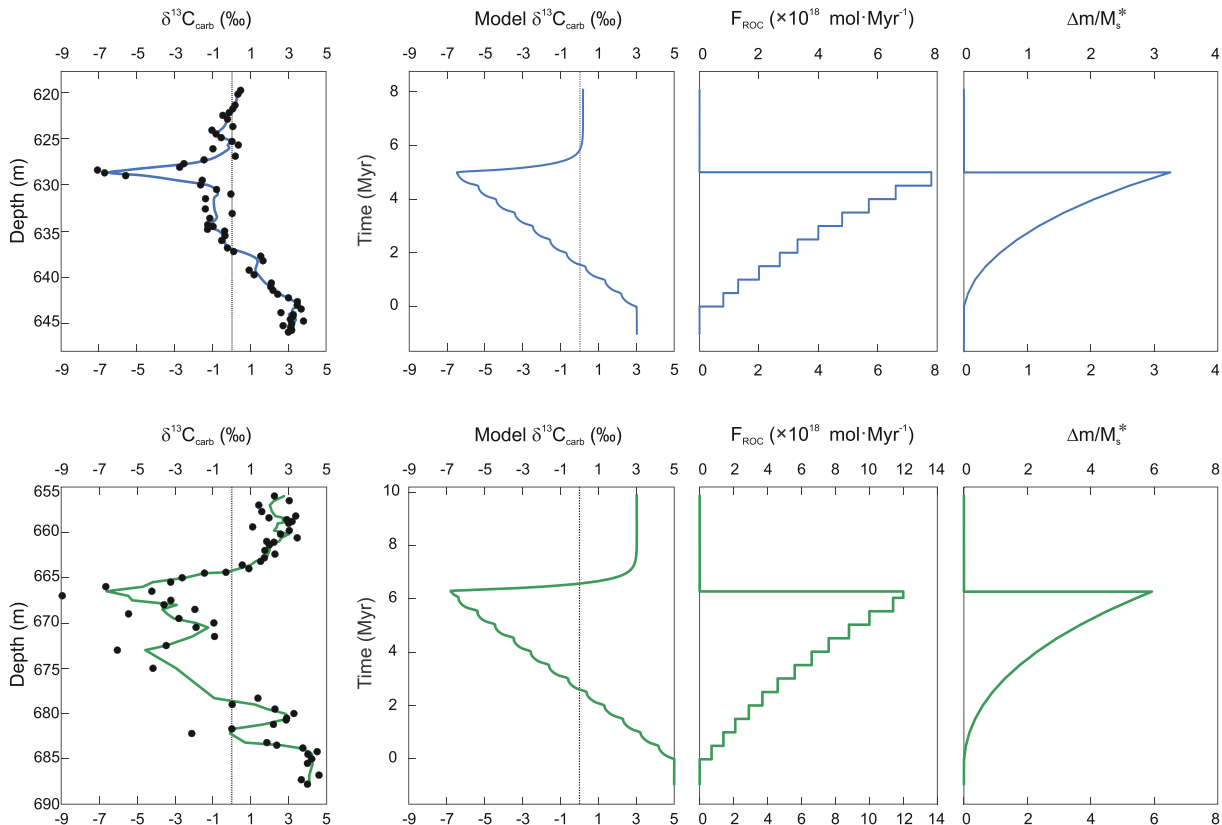


**Fig. 11.** Comparison of the observed (three-point average) and modeled C isotope compositions in phosphorite-rich units in the Doushantuo Formation and model predictions of  $F_{ROC}$  and  $\Delta m/M_s^*$  (the mass of remineralized DIC normalized by the initial DIC mass of the surface ocean). Time ( $t$ ) is estimated by the deposition rate.

and had a major impact on the seawater chemistry of the surface ocean. Importantly, large amounts of DOC were carried from deep to surface areas by upwelling, which fundamentally changed the global carbon cycle. Using piecewise functions,  $\sim 3.6 \times 10^{19}$  mol and  $\sim 2.0 \times 10^{19}$  mol DOC were oxidized to DIC in surface regions during the two negative  $\delta^{13}\text{C}_{\text{carb}}$  excursions. These estimates are approximately 1000 times the total amount of modern marine DOC reservoirs<sup>[45]</sup>.

It is debated whether the oxidant was sufficient to sustain the negative C-isotopic excursion of such magnitude during the Ediacaran Period. The oxidation of DOC is fueled by the consumption of oxygen or sulfate<sup>[46]</sup>. Our model results show that  $\sim 3.6 \times 10^{19}$  mol and  $\sim 2.0 \times 10^{19}$  mol free oxygen (compared to the modern  $\text{O}_2$  reservoir of  $\sim 3.6 \times 10^{19}$  mol) were needed to sustain the C isotopic excursion of  $-12\text{‰}$  (684.2–660.6 m) and  $-10\text{‰}$  (642.2–621.8 m), respectively. The shelf region, where the sediments of the Wangji drill core were deposited, may provide excellent sites for organic-rich sediment burial, as high biological primary productivity was likely maintained for millions of years with surplus upwelled nutrients (e.g., phosphorus)<sup>[28, 29, 33]</sup>. Additionally, a thick layer of organic-rich black shale overlying the Doushantuo cap carbonate is widespread across the whole of South China, extending from north to south for more than 500 km, which also suggests the increased burial of organic carbon and release of  $\text{O}_2$ <sup>[47]</sup>.

Sulfate may represent another potential oxidant capable of mineralizing organic carbon in the ocean. Based on the model,  $\sim 1.9 \times 10^{19}$  mol and  $\sim 0.8 \times 10^{19}$  mol sulfate (compared to the modern sulfate reservoir of  $\sim 4 \times 10^{19}$  mol) are needed to sustain the two negative C-isotopic excursions, respectively. Shields et al.<sup>[48]</sup> proposed basin-scale evaporite dissolution as an important oxidant source for the Ediacaran DOC reservoir. Therefore, considering the evidence from previous studies<sup>[28, 29, 33, 47, 48]</sup>, both  $\text{O}_2$  and sulfate may have had a significant impact on the oxidation of the DOC reservoir.

Our simulation results have two important implications. First, the DOC reservoir in the late Neoproterozoic was likely much larger than previously thought, and thus the DOC buffering effect could have led to globally decoupled paired carbon isotopic records ( $\delta^{13}\text{C}_{\text{carb}}$  and  $\delta^{13}\text{C}_{\text{org}}$ ). Second, the atmospheric oxygen content and/or oceanic sulfate concentration could have already risen to a relatively high level in the early Ediacaran Period, given the high oxidation capacity of the Earth's surface.

## 6 Conclusions

The Ediacaran oceans were likely to be rather dynamic in terms of the existence of strong upwelling water masses. Upwelling not only linked anoxic deep oceans and oxic surface regions, but also provided large quantities of nutrients (e.g., phosphorous) for the pelagic primary producers that released free  $\text{O}_2$ . The DOC reservoir may have greatly decreased during the Ediacaran Period, and both ecosystems (e.g., cyanobacteria and algae) and the environment ( $p\text{O}_2$  and/or  $[\text{SO}_4^{2-}]$  rise) may have played a role. Stepwise oxygenation of the Earth's surface in the late Neoproterozoic may have created the necessary external conditions for the Ediacaran biota, paving the way for subsequent macroscopic animal evolution.

## Acknowledgements

We thank the anonymous reviewers for their constructive comments. This work is supported by the National Natural Science Foundation of China (42003058), China Postdoctoral Science Foundation (2021M703058), and the Fundamental Research Funds for the Central Universities (WK2080000136, WK2080000148).

## Conflict of interest

The authors declare that they have no conflict of interest.

## Biographies

**Yunpei Gao** received his BS and PhD degrees from University of Science and Technology of China (USTC) in 2013 and 2020, respectively. He is now a postdoctoral researcher at USTC. His areas of interest include paleoenvironmental reconstruction, the global carbon cycle, and biogeochemical processes.

**Xiaoyan Chen** received her BS and PhD degree in Geochemistry from University of Science and Technology of China in 2013 and 2020, respectively. Her research interests mainly focus on redox conditions and biogeochemical cycles of carbon and sulfur in the Meso- and Neoproterozoic oceans.

## References

- [1] Farquhar J, Bao H, Thieme M. Atmospheric influence of Earth's earliest sulfur cycle. *Science*, **2000**, 289 (5480): 756–758.
- [2] Fike D A, Grotzinger J P, Pratt L M, et al. Oxidation of the Ediacaran ocean. *Nature*, **2006**, 444 (7120): 744–747.
- [3] Holland H D. The oxygenation of the atmosphere and oceans. *Phil Trans R Soc B*, **2006**, 361 (1470): 903–915.
- [4] Frei R, Gaucher C, Poulton S W, et al. Fluctuations in Precambrian atmospheric oxygenation recorded by chromium isotopes. *Nature*, **2009**, 461 (7261): 250–253.
- [5] Och L M, Shields-Zhou G A. The Neoproterozoic oxygenation event: Environmental perturbations and biogeochemical cycling. *Earth-Science Reviews*, **2012**, 110 (1–4): 26–57.
- [6] Sahoo S K, Planavsky N J, Kendall B, et al. Ocean oxygenation in the wake of the Marinoan glaciation. *Nature*, **2012**, 489 (7417): 546–549.
- [7] Lyons T W, Reinhard C T, Planavsky N J. The rise of oxygen in Earth's early ocean and atmosphere. *Nature*, **2014**, 506 (7488): 307–315.
- [8] Luo G, Ono S, Beukes N J, et al. Rapid oxygenation of Earth's atmosphere 2.33 billion years ago. *Science Advances*, **2016**, 2 (5): e1600134–e1600134.
- [9] Gumsley A P, Chamberlain K R, Bleeker W, et al. Timing and tempo of the Great Oxidation Event. *Proc Natl Acad Sci USA*, **2017**, 114 (8): 1811–1816.
- [10] Pavlov A A, Kasting J F. Mass-independent fractionation of sulfur isotopes in Archean sediments: Strong evidence for an anoxic Archean atmosphere. *Astrobiology*, **2002**, 2 (1): 27–41.
- [11] Farquhar J, Wing B A. Multiple sulfur isotopes and the evolution of the atmosphere. *Earth and Planetary Science Letters*, **2003**, 213: 1–13.
- [12] Hardisty D S, Lu Z, Planavsky N J, et al. An iodine record of Paleoproterozoic surface ocean oxygenation. *Geology*, **2014**, 42 (7): 619–622.
- [13] McFadden K A, Huang J, Chu X, et al. Pulsed oxidation and biological evolution in the Ediacaran Doushantuo Formation. *Proc Natl Acad Sci USA*, **2008**, 105 (9): 3197–3202.



- [14] Papineau D. Global biogeochemical changes at both ends of the proterozoic: Insights from phosphorites. *Astrobiology*, **2010**, *10* (2): 165–181.
- [15] Planavsky N J, Rouxel O J, Bekker A, et al. The evolution of the marine phosphate reservoir. *Nature*, **2010**, *467* (7319): 1088–1090.
- [16] Brocks J J, Jarrett A J M, Sirantoine E, et al. The rise of algae in Cryogenian oceans and the emergence of animals. *Nature*, **2017**, *548* (7669): 578–581.
- [17] Butterfield N J. Oxygen, animals and oceanic ventilation: An alternative view. *Geobiology*, **2009**, *7* (1): 1–7.
- [18] Rothman D H, Hayes J M, Summons R E. Dynamics of the Neoproterozoic carbon cycle. *Proc Natl Acad Sci USA*, **2003**, *100* (14): 8124–8129.
- [19] Hoefs J. *Stable Isotope Geochemistry*. Sixth edition. Berlin: Springer-Verlag, 2009: 48–53.
- [20] Kump L R, Arthur M A. Interpreting carbon-isotope excursions: Carbonates and organic matter. *Chemical Geology*, **1999**, *161* (1–3): 181–198.
- [21] Hayes J M, Strauss H, Kaufman A J. The abundance of  $^{13}\text{C}$  in marine organic matter and isotopic fractionation in the global biogeochemical cycle of carbon during the past 800 Ma. *Chemical Geology*, **1999**, *161* (1–3): 103–125.
- [22] Halverson G P, Hoffman P F, Schrag D P, et al. Toward a Neoproterozoic composite carbon-isotope record. *Geological Society of America Bulletin*, **2005**, *117* (9–10): 1181–1207.
- [23] Swanson-Hysell N L, Rose C V, Calmet C C, et al. Cryogenian glaciation and the onset of carbon-isotope decoupling. *Science*, **2010**, *328* (5978): 608.
- [24] Schrag D P, Higgins J A, Macdonald F A, et al. Authigenic carbonate and the history of the global carbon cycle. *Science*, **2013**, *339* (6119): 540–543.
- [25] Sun X, Turchyn A V. Significant contribution of authigenic carbonate to marine carbon burial. *Nature Geoscience*, **2014**, *7* (3): 201–204.
- [26] Cui H, Xiao S, Zhou C, et al. Phosphogenesis associated with the Shuram Excursion: Petrographic and geochemical observations from the Ediacaran Doushantuo Formation of South China. *Sedimentary Geology*, **2016**, *341*: 134–146.
- [27] Cui H, Kaufman A J, Xiao S, et al. Was the Ediacaran Shuram Excursion a globally synchronized early diagenetic event? Insights from methane-derived authigenic carbonates in the uppermost Doushantuo Formation, South China. *Chemical Geology*, **2017**, *450*: 59–80.
- [28] Gao Y, Zhang X L, Zhang G J, et al. Ediacaran negative C-isotopic excursions associated with phosphogenic events: Evidence from South China. *Precambrian Research*, **2018**, *307*: 218–228.
- [29] Gao Y, Zhang X, Xu Y, et al. High primary productivity during the Ediacaran Period revealed by the covariation of paired C-isotopic records from South China. *Precambrian Research*, **2020**, *349*: 105411.
- [30] Li Z X, Li X H, Kinny P D, et al. The breakup of Rodinia: Did it start with a mantle plume beneath South China? *Earth and Planetary Science Letters*, **1999**, *173* (3): 171–181.
- [31] Wang J, Li Z. History of Neoproterozoic rift basins in South China: implications for Rodinia break-up. *Precambrian Research*, **2003**, *122* (1–4): 141–158.
- [32] Jiang G, Shi X, Zhang S, et al. Stratigraphy and paleogeography of the Ediacaran Doushantuo Formation (ca. 635–551 Ma) in South China. *Gondwana Research*, **2011**, *19* (4): 831–849.
- [33] Gao Y, Zhang X, Fang C, et al. Reconstruction of the Ediacaran sulfur cycle and oceanic redox evolution in shallow-water regions of the Yangtze platform, South China. *Precambrian Research*, **2021**, *353*: 106004.
- [34] Condon D, Zhu M, Bowring S, et al. U-Pb ages from the Neoproterozoic Doushantuo Formation, China. *Science*, **2005**, *308* (5718): 95–98.
- [35] Chen D, Zhou X, Fu Y, et al. New U-Pb zircon ages of the Ediacaran-Cambrian boundary strata in South China. *Terra Nova*, **2015**, *27* (1): 62–68.
- [36] Jiang G, Kaufman A J, Christie-Blick N, et al. Carbon isotope variability across the Ediacaran Yangtze platform in South China: Implications for a large surface-to-deep ocean  $\delta^{13}\text{C}$  gradient. *Earth and Planetary Science Letters*, **2007**, *261* (1–2): 303–320.
- [37] Zhou C, Xiao S. Ediacaran  $\delta^{13}\text{C}$  chemostratigraphy of South China. *Chemical Geology*, **2007**, *237* (1–2): 89–108.
- [38] Zhu M, Lu M, Zhang J, et al. Carbon isotope chemostratigraphy and sedimentary facies evolution of the Ediacaran Doushantuo Formation in western Hubei, South China. *Precambrian Research*, **2013**, *225*: 7–28.
- [39] Wang X, Jiang G, Shi X, et al. Paired carbonate and organic carbon isotope variations of the Ediacaran Doushantuo Formation from an upper slope section at Siduping, South China. *Precambrian Research*, **2016**, *273*: 53–66.
- [40] Nichols G. *Sedimentology and Stratigraphy*. Second edition. Chichester, West Sussex, UK: Wiley-Blackwell, 2009: 28–43.
- [41] Kump L R. Interpreting carbon-isotope excursions: Strangelove oceans. *Geology*, **1991**, *19* (4): 299–302.
- [42] Zhang G, Zhang X, Shen Y. Quantitative constraints on carbon cycling and temporal changes in episodic euxinia during the end-Permian mass extinction in South China. *Chemical Geology*, **2021**, *562*: 120036.
- [43] Shi W, Li C, Algeo T J. Quantitative model evaluation of organic carbon oxidation hypotheses for the Ediacaran Shuram carbon isotopic excursion. *Science China Earth Sciences*, **2017**, *60* (12): 2118–2127.
- [44] Gill B C, Lyons T W, Young S A, et al. Geochemical evidence for widespread euxinia in the Later Cambrian ocean. *Nature*, **2011**, *469* (7328): 80–83.
- [45] Fakrae M, Tarhan L G, Planavsky N J, et al. A largely invariant marine dissolved organic carbon reservoir across Earth's history. *Proc Natl Acad Sci USA*, **2021**, *118* (40): e2103511118.
- [46] Bristow T F, Kennedy M J. Carbon isotope excursions and the oxidant budget of the Ediacaran atmosphere and ocean. *Geology*, **2008**, *36*: 863–866.
- [47] Jiang G, Wang X, Shi X, et al. Organic carbon isotope constraints on the dissolved organic carbon (DOC) reservoir at the Cryogenian–Ediacaran transition. *Earth and Planetary Science Letters*, **2010**, *299*: 159–168.
- [48] Shields G A, Mills B J W, Zhu M, et al. Unique Neoproterozoic carbon isotope excursions sustained by coupled evaporite dissolution and pyrite burial. *Nature Geoscience*, **2019**, *12*: 823–827.